# Electronic Supplementary Information

# Design of efficient bifunctional catalysts for direct conversion of syngas into lower olefins via methanol/dimethyl ether intermediates

Xiaoliang Liu,[a] Wei Zhou,[a] Yudan Yang,[a] Kang Cheng,*[a] Jincan Kang,[a] Lei Zhang,[b] Guoquan Zhang,[b] Xiaojian Min,[b] Qinghong Zhang*[a] and Ye Wang*[a]

[a]*State Key Laboratory of Physical Chemistry of Solid Surfaces, Collaborative Innovation Center of Chemistry for Energy Materials, National Engineering Laboratory for Green Chemical Productions of Alcohols, Ethers and Esters, College of Chemistry and Chemical Engineering, Xiamen University, Xiamen 361005, P. R. China.*

[b]*State Energy Key Lab of Clean Coal Grading Conversion, Shaanxi Coal and Chemical Technology Institute Co., Ltd., Xi'an 710070, P. R. China.*

## 1. Experimental details

### 1.1 Catalyst preparation

The micro-sized Na-SSZ-13 (Si/Al = 7.5, atomic ratio) was purchased from Shanghai Saint Chemical Materials Co. Ltd. The Na-type samples were exchanged into their H-type forms by the ion-exchanging method using 1.0 M $NH_4NO_3$ aqueous solution. In brief, 1.0 g Na-SSZ-13 powder was added into 100 mL $NH_4NO_3$ aqueous solution at 353 K, followed by stirring for 3 h. The obtained sample was washed with deionized water and calcined at 823 K in air for 6 h. The exchanging procedure was performed for 3 times. The SSZ-13 samples with different $H^+$-exchanging degrees were prepared by a similar procedure. The concentration of aqueous $NH_4NO_3$ solution was varied in a range of 0.01-1.0 M to regulate the $H^+$-exchanging degree. The SSZ-13 sample with an $H^+$-exchanging degree of *x* was denoted as SSZ-13-*x*H. The SSZ-13-45H was typically used for the preparation of bifunctional catalysts unless otherwise mentioned.

The nano-sized SSZ-13 was synthesized by a hydrothermal method from a gel with composition of ($Na_2O/SiO_2/Al_2O_3$/*N*,*N*,*N*-trimethyl-1-adamantanammoniumhydroxide (TMAdOH)/$H_2O$ = 0.1/1/0.067/0.2/44, molar ratio).[1] TMAdOH was first mixed with NaOH and deionized water at room temperature until it was dissolved completely. Then, aerosil $SiO_2$ and $Al_2O_3$ were added to the solution. The mixture was stirred at room temperature for 1 h to obtain a homogeneous gel, which was then transferred into a Teflon-lined stainless-steel autoclave and kept statically in an oven at 433 K for 24 h. After that, hexadecyltrimethylammonium bromide (CTAB, molar ratio of CTAB/$SiO_2$ = 0.12) as a modifier was mixed completely with the solution. The resulting gel containing CTAB was transferred into the Teflon-lined autoclave again and heated at 433 K for 9 days. The product was recovered by filtration, washing with deionized water and drying at 373 K. The solid powders were calcined at 823 K in air to remove the organic template or modifier. The obtained Na-type nano-sized SSZ-13 was ion-exchanged to obtain the product with optimized density of Brønsted acid sites using $NH_4NO_3$ aqueous solution as described above.

The Zn-doped $ZrO_2$ (denoted as Zn–$ZrO_2$) was synthesized with a sol-gel method.[2] In a typical procedure, $Zr(NO_3)_4{\cdot}5H_2O$, $Zn(NO_3)_2{\cdot}6H_2O$ and citric acid were dissolved in 100 mL deionized water. The mixture was evaporated at 363 K until a viscous gel was obtained. Then, the mixture was heated to 453 K for 3 h and calcined at 773 K in air for 5 h. The obtained sample was denoted as Zn–$ZrO_2$ (*m*:*n*), where *m*:*n* was the molar ratio of Zn/Zr. The Zn–$ZrO_2$ (1:16) with a mean diameter of 8.9 nm was typically used for the preparation of bifunctional catalyst unless otherwise specified.

The Zn–$ZrO_2$ (1:16) sample with a mean size of 4.8 nm was synthesized using a method reported previously.[3] Briefly, zirconium (IV), Zn(II) and *n*-propoxide were dissolved in 15 mL *n*-propanol containing 1.9 mL $HNO_3$ (70 wt%). A mixture of 1.3 mL $H_2O$ and 15 mL *n*-propanol solution was added into the system descried above under vigorous stirring until a colloidal solid was generated. To remove *n*-propanol solvent completely, the gel was packed into a kettle and extracted by supercritical $CO_2$ flow at 333 K and 15 MPa. The dried powder was calcined in air flow at 773 K for 5 h.

For comparison, a Cu-Zn-Al (Cu/Zn/Al = 6:3:1, molar ratio) mixed oxide was prepared

by a co-precipitation method. Briefly, an aqueous solution of metal nitrates [$Cu(NO_3)_2 \cdot 3H_2O$ (0.6 M), $Zn(NO_3)_2 \cdot 6H_2O$ (0.3 M), and $Al(NO_3)_3 \cdot 9H_2O$ (0.1 M)] and an aqueous solution of $Na_2CO_3$ (1.0 M) as precipitating agent were simultaneously added to a glass beaker under stirring at 343 K and a pH of 7.0. Once the addition of the metal nitrate solution finished, the suspension was aged for 2 h at the same temperature while keeping the pH constant at 7.0 through addition of nitrate or $Na_2CO_3$ solution. Subsequently, the precipitate was filtered, washed with deionized water, dried in an oven at 373 K for 12 h and finally calcined at 573 K under air flow for 3 h.

The bifunctional catalysts were prepared by a simple mortar-mixing method. The weight ratio of Zn–$ZrO_2$ and SSZ-13 was fixed at 1:2 in the present work. Briefly, powders of Zn–$ZrO_2$ and SSZ-13 were grinded in an agate mortar for 10 min. The obtained catalyst was denoted as Zn–$ZrO_2$/SSZ-13.

For the preparation of Zn–$ZrO_2$/SSZ-13 with granules stacking together, the samples of Zn–$ZrO_2$ and SSZ-13 were pressed separately, crushed and sieved to 30-60 meshes (granule sizes of 250-600 μm). Then, the granules of the two samples with sizes of 250-600 μm were mixed homogeneously by shaking in a vessel.

### 1.2 Catalyst characterization

X-ray powder diffraction (XRD) patterns were recorded on a Rigaku Ultima IV diffractometer. The Cu $K_\alpha$ radiation ($\lambda$ = 0.15406 nm) generated at 40 kV and 30 mA was used as the X-ray source. The mean size of $ZrO_2$ crystallites was estimated by the Scherrer equation using a [011] tetragonal $ZrO_2$ XRD peak at a $2\theta$ of 30.3°.

$N_2$ physisorption measurements were performed on a Micromeritics Tristar II 3020 Surface Area Analyzer. Prior to $N_2$ adsorption, the sample was degassed under vacuum at 473 K for 3 h.

Scanning electron microscopy (SEM) measurements were performed on a Hitachi S-4800 operated at 15 kV. The sample was dispersed ultrasonically in ethanol for 10 min, and then was dropped onto a silicon pellet, followed by drying for 60 min. Transmission electron microscopy (TEM) measurements were carried out on a Phillips Analytical FEI Tecnai20

electron microscope operated at an acceleration voltage of 200 kV. The sample was dispersed ultrasonically in ethanol for 5 min, and a drop of solution was deposited onto a carbon-coated copper grid. More than 200 particles were used to evaluate the mean particle size from TEM images.

$NH_3$ temperature-programmed desorption ($NH_3$-TPD) measurements were performed on a Micromeritics AutoChemII 2920 instrument. Typically, the sample was pretreated in a quartz reactor with an $O_2$-He gas (20 vol% $O_2$) flow at 673 K for 1 h, followed by purge with high-purity He. The adsorption of $NH_3$ was performed at 373 K in an $NH_3$-He mixture (10 vol% $NH_3$) for 1 h, and TPD was performed in He flow by raising the temperature to 1173 K at a rate of 10 K $min^{-1}$.

Fourier-transform infrared (FT-IR) studies of adsorbed $NH_3$ were carried out on a Nicolet 6700 instrument equipped with an MCT detector. The sample was pressed into a self-supported wafer and placed in an *in situ* IR cell. After pretreated under vacuum at 673 K for 30 min, the sample was cooled down to 373 K. Then, $NH_3$ was adsorbed at 373 K on the sample for a sufficient time. FT-IR spectra were recorded after gaseous or weakly adsorbed $NH_3$ molecules were removed by evacuation at 373 K. For quantification of Brønsted acid sites, molar extinction coefficient ($\varepsilon_B = 0.147$ $cm^2$ $\mu mol^{-1}$) of $NH_3$ band at 1400 $cm^{-1}$ and 1450 $cm^{-1}$ was used.[4-6]

*In situ* diffuse reflection infrared Fourier-transform spectroscopy (DRIFTS) measurements were performed on a Nicolet 6700 instrument equipped with an MCT detector. *In situ* absorbance spectra were obtained by collecting 120 scans at 4 $cm^{-1}$ resolution. Before measurement, catalyst was pretreated with Ar flow at 673 K for 1 h. Subsequently, the catalyst was cooled down to the test temperature. The information of surface hydroxyl groups was obtained at 323 K by subtracting the background of KBr. To gain information on surface species during reactions, the catalyst was first exposed to CO for 30 min at 553 K, followed by switching to $CO/H_2$ gas. The evolution of surface species was recorded at different times.

### 1.3 Catalytic reaction

The conversion of syngas was performed on a high-pressure fixed-bed reactor built by Xiamen HanDe Engineering Co., Ltd. Typically, 0.60 g catalyst with grain sizes of 250-600 μm (30-60 mesh) was loaded in a titanium reactor (inner diameter, 10 mm). Syngas with a $H_2$/CO ratio of 2:1 and a pressure of 3.0 MPa was introduced into the reactor. Argon with a concentration of 4.0% in the syngas was used as an internal standard for the calculation of CO conversion. The temperature was raised to the desired reaction temperature (typically 673 K) to start the reaction. The catalytic conversion of methanol was performed with the same reactor. The pressure of $H_2$ was raised to 2.0 MPa with a flow rate of 30 mL $min^{-1}$ and the temperature was raised to the desired reaction temperature (typically 673 K). After that, methanol was introduced into the reactor by a Series II pump in the presence of $H_2$ flow to start the reaction. For both reactions, products were analyzed by an online gas chromatograph, which was equipped with a thermal conductivity detector (TCD) and a flame ionization detector (FID). A TDX-01 packed column was connected to TCD, while a RT-Q-BOND-PLOT capillary column was connected to FID. The selectivity presented in this work was calculated on a molar carbon basis for CO hydrogenation (without considering $CO_2$). Carbon balances were all better than 95%. The selectivity of $CO_2$ was calculated separately. The catalytic performance after 10 h of reaction was typically used for discussion.

## 2. Interpretation of rate equation from kinetic analysis by Langmuir-Hinshelwood mechanism

Our studies have pointed out that the whole reaction is rate-limited by the conversion of syngas over the Zn−$ZrO_2$ catalyst. As proposed in Fig. 13, CO is adsorbed on $ZrO_2$ surfaces, while $H_2$ is dissociatively adsorbed on −Zn−O− domains (or ZnO clusters) incorporated in or located on $ZrO_2$. We assume that the surface reaction between the adsorbed CO and the dissociatively adsorbed H species, which follows a dual-site Langmuir-Hinshelwood mechanism, is the rate-determining step. Then, we can express the rate equation as:

$$r(\mathrm{CO}) = k\theta(\mathrm{CO})\theta(\mathrm{H})$$

where $\theta$(CO) and $\theta$(H) are surface coverages of adsorbed CO and H species. According to Langmuir adsorption model, the surface coverages of adsorbed CO and H species can be calculated as:

$$\theta(\mathrm{CO}) = \frac{K(\mathrm{CO})P(\mathrm{CO})}{1 + K(\mathrm{CO})P(\mathrm{CO})}$$

$$\theta(H) = \frac{K(\mathrm{H_2})^{1/2}P(\mathrm{H_2})^{1/2}}{1 + K(\mathrm{H_2})^{1/2}P(\mathrm{H_2})^{1/2}}$$

where $K$(CO) and $K$($H_2$) are the adsorption equilibrium constants of CO and $H_2$. Thus, the rate equation can be expressed as:

$$r(\mathrm{CO}) = k\frac{K(\mathrm{CO})P(\mathrm{CO})}{[1 + K(\mathrm{CO})P(\mathrm{CO})]}\frac{K(\mathrm{H_2})^{1/2}\,P(\mathrm{H_2})^{1/2}}{[1 + K(\mathrm{H_2})^{1/2}P(\mathrm{H_2})^{1/2}]}$$

where $k$ is the rate constant. This equation is the same as that obtained from kinetic experiments (Eq. 4).

## 3. Supplementary Figures and Tables

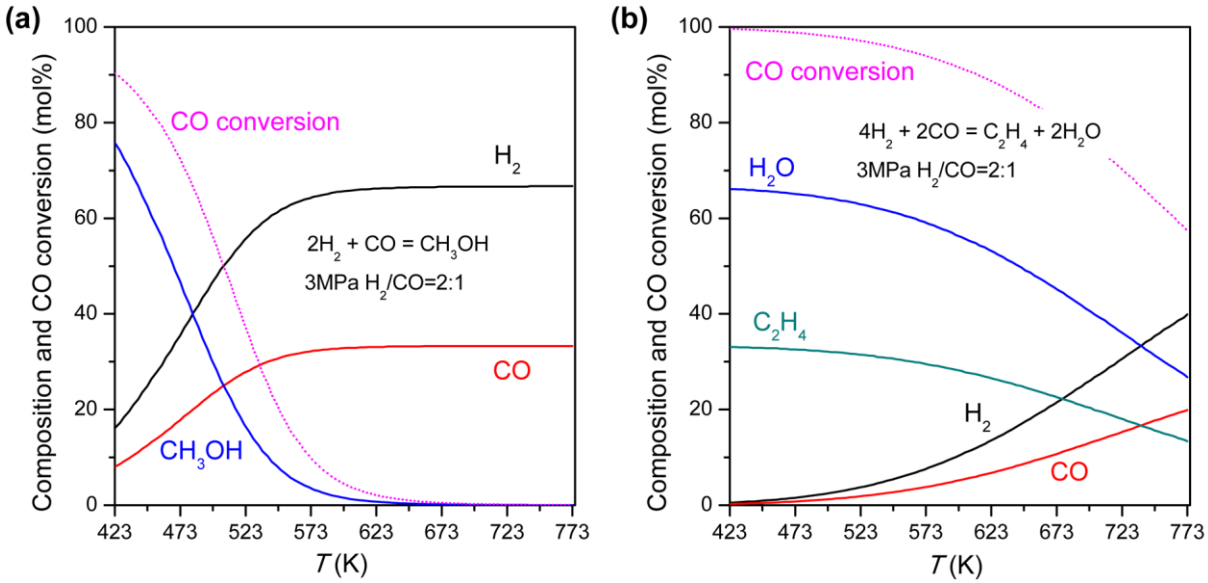


**Fig. S1** Equilibrium composition and CO conversion during the synthesis of methanol (a) and ethylene (b) via hydrogenation of CO. Simulated conditions: $H_2/CO$ = 2 and $P$ = 3 MPa. The calculation was based on HSC5 chemistry software.

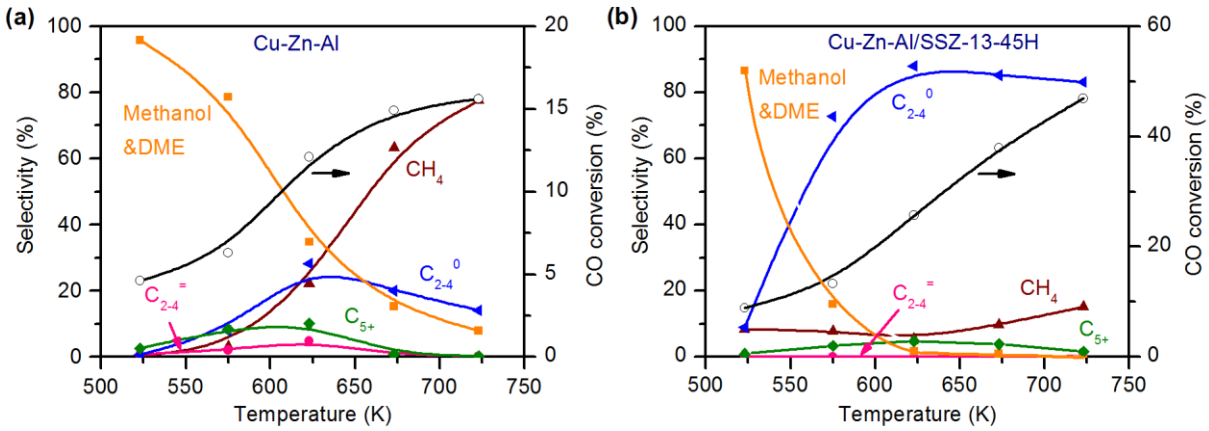


**Fig. S2** Catalytic performances of Cu-Zn-Al and Cu-Zn-Al/SSZ-13-45H for the conversion of syngas at different temperatures. (a) Cu-Zn-Al (Cu/Zn/Al = 6/3/1, molar ratio); (b) Cu-Zn-Al/SSZ-13-45H. Reaction conditions: $W$ (Cu-Zn-Al) = 0.20 g; $W$ (Cu-Zn-Al/SSZ-13-45H) = 0.60 g; $H_2/CO$ = 2; $P$ = 3 MPa; $F$ = 30 mL $min^{-1}$; time on stream, 10 h.

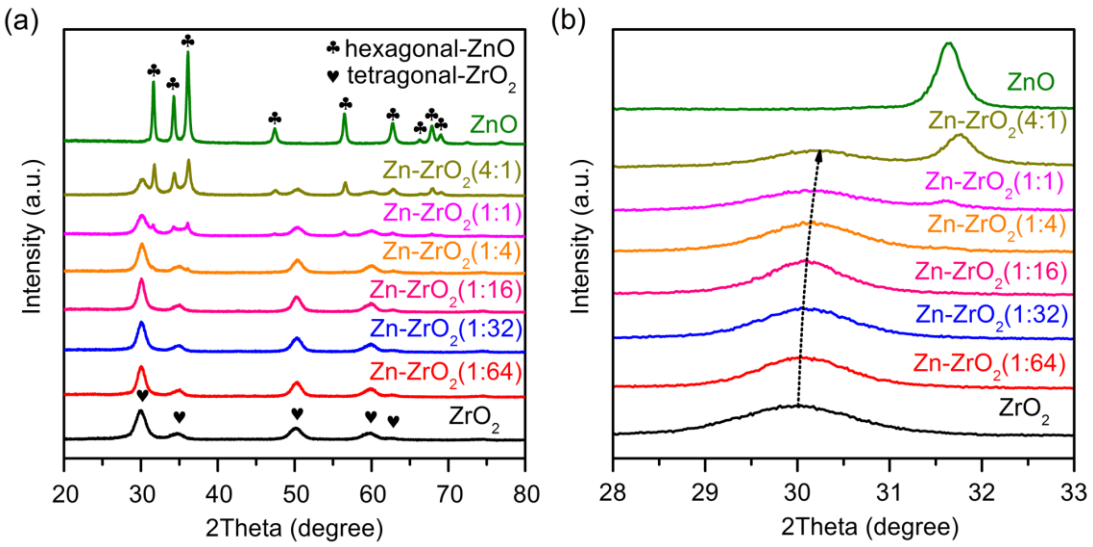


**Fig. S3** XRD patterns of Zn−$ZrO_2$ catalysts with different Zn/Zr molar ratios as well as $ZrO_2$ and ZnO. (a) $2\theta$ at 20-80º. (b) $2\theta$ at 28-33º.

The [011] peak of tetragonal $ZrO_2$ slightly shifted to higher angles after the doping of ZnO. This shift is probably caused by the incorporation of ZnO into $ZrO_2$ matrix.

**Table S1.** Structural properties of Zn−$ZrO_2$ samples with different Zn/Zr ratios.

| Sample | $S_{BET}$[a] ($m^2\ g^{-1}$) | $V_{tot}$[b] ($cm^3\ g^{-1}$) | $ZrO_2$ size[c] (nm) | Particle size[d] (nm) |
|---|---|---|---|---|
| $ZrO_2$ | 85 | 0.11 | 6.0 | 6.6 ± 0.9 |
| Zn−$ZrO_2$ (1:64) | 79 | 0.14 | 7.3 | 6.8 ± 1.3 |
| Zn−$ZrO_2$ (1:32) | 75 | 0.08 | 7.1 | 8.0 ± 1.4 |
| Zn−$ZrO_2$ (1:16) | 62 | 0.08 | 7.3 | 8.9 ± 1.6 |
| Zn−$ZrO_2$ (1:4) | 50 | 0.08 | 7.4 | 9.9 ± 1.7 |
| Zn−$ZrO_2$ (1:1) | 54 | 0.10 | 7.0 | 9.5 ± 1.5 |
| Zn−$ZrO_2$ (4:1) | 45 | 0.08 | 7.5 | 14 ± 5.2 |
| ZnO | 9.4 | 0.09 | 27[e] | 45 ± 14 |

[a] BET surface area.

[b] Single point desorption total pore volume, $P/P_0 = 0.99$.

[c] The size of $ZrO_2$ crystallite was estimated from XRD peak at $2\theta = 30.3$º using the Scherrer equation.

[d] The mean size of particles were obtained from TEM measurements.

[e] The size of ZnO crystallite was estimated from XRD peak at $2\theta = 36.3$º using the Scherrer equation.

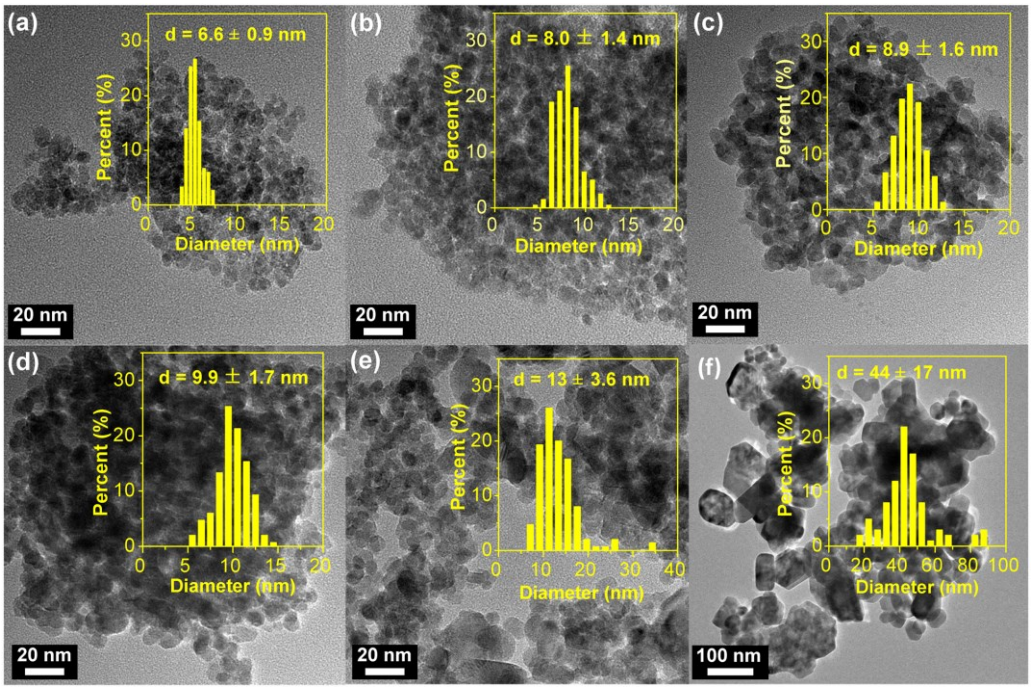


**Fig. S4** TEM micrographs for Zn−$ZrO_2$ samples with different Zn/Zr ratios. Zn/Zr molar ratio: (a) 0, (b) 1:32, (c) 1:16, (d) 1:4, (e) 4:1, (f) ZnO.

**Table S2.** The density of acid sites for SSZ-13 samples obtained from $NH_3$-TPD and $NH_3$-FT-IR.

| Catalysts | Density of strong acid sites[a] (mmol $g^{-1}$) | Density of Brønsted acid sites[b] (mmol $g^{-1}$) |
|---|---|---|
| SSZ-13-100H | 0.23 | 0.19 |
| SSZ-13-70H | 0.16 | 0.14 |
| SSZ-13-63H | 0.15 | 0.14 |
| SSZ-13-53H | 0.12 | - |
| SSZ-13-45H | 0.10 | 0.08 |
| SSZ-13-30H | 0.07 | - |
| SSZ-13-18H | 0.04 | 0.04 |
| SSZ-13-8H | 0.02 | - |
| SSZ-13-0H | 0 | 0 |

[a] The density of strong acid sites was evaluated from the high-temperature $NH_3$-TPD peak.

[b] The density of Brønsted acid sites was evaluated from the $NH_3$-FT-IR bands at 1400 $cm^{-1}$ and 1450 $cm^{-1}$ together.[6]

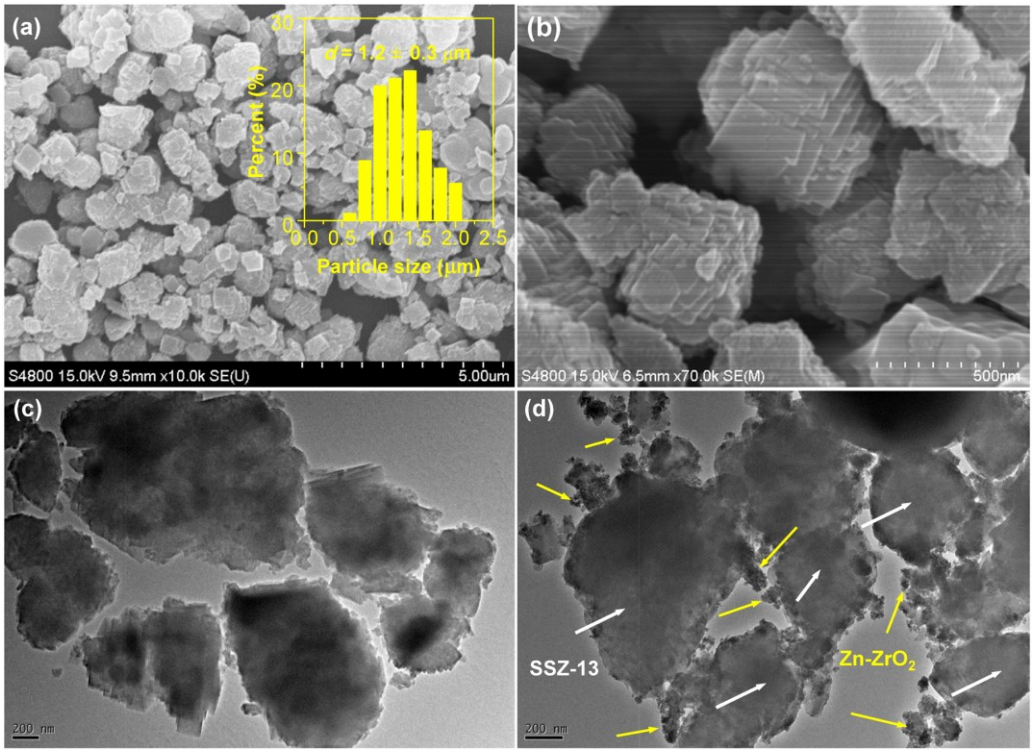


**Fig. S5** (a, b) SEM and (c) TEM images of the micro-sized SSZ-13-45H zeolite. (d) TEM image of Zn–$ZrO_2$/SSZ-13-45H.

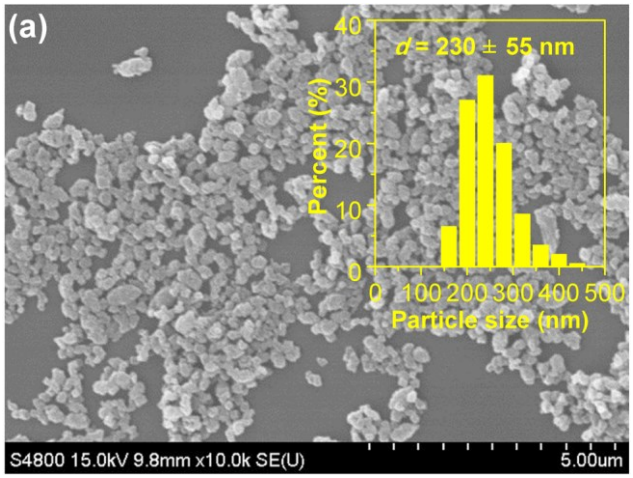


**Fig. S6** SEM image of nano-sized SSZ-13 with particle size distribution.

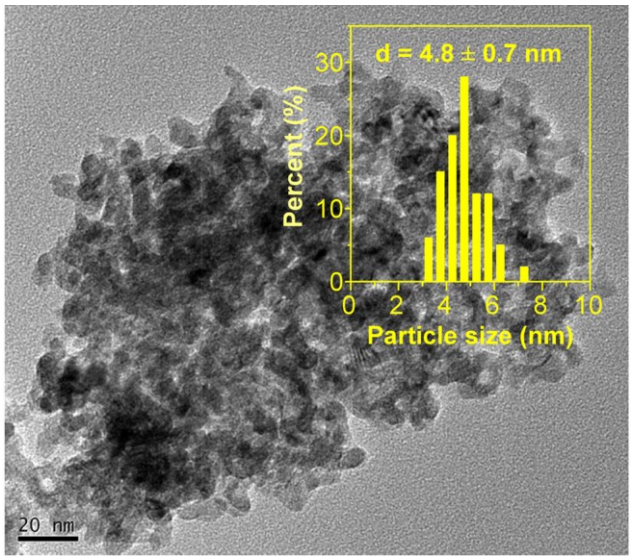


**Fig. S7** TEM image of Zn−$ZrO_2$ particles with particle size distribution.

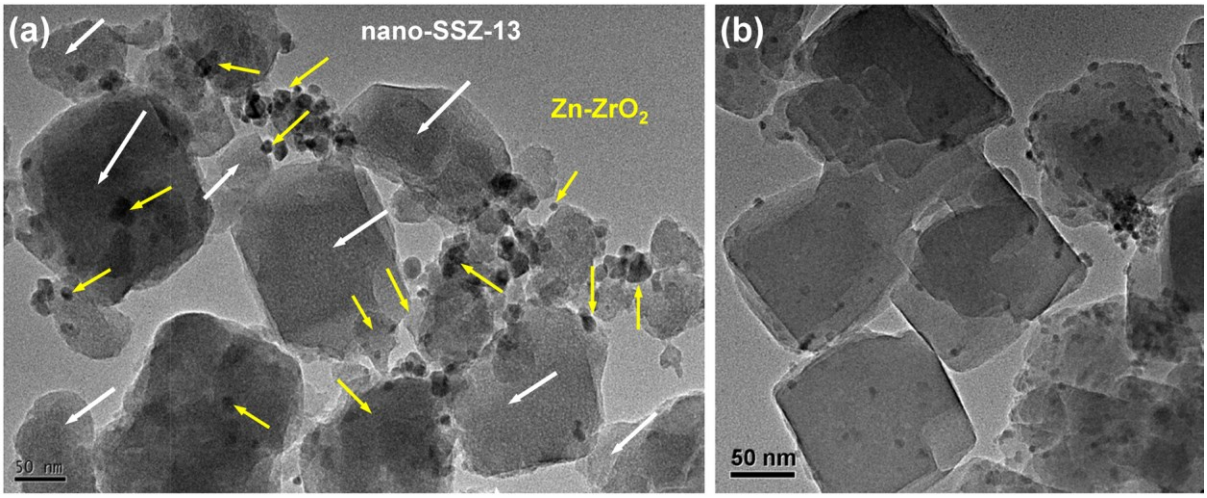


**Fig. S8** (a) Zn−$ZrO_2$/nano-SSZ-13 with a mean size of Zn−$ZrO_2$ particles of 8.9 nm. (b) Zn−$ZrO_2$/nano-SSZ-13 with a mean size of Zn−$ZrO_2$ particles of 4.8 nm.

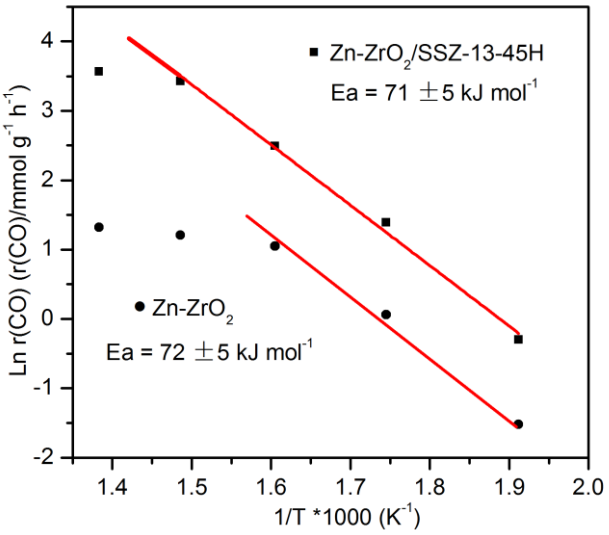


**Fig. S9** Logarithms of CO conversion rate versus the reciprocal of temperature for the conversion of syngas to methanol (circle symbols) over Zn–$ZrO_2$ and the conversion of syngas to lower olefins (square symbols) over Zn–$ZrO_2$/SSZ-13-45H. Reaction conditions: $W$(Zn–$ZrO_2$) = 0.20 g; $W$(Zn–$ZrO_2$/SSZ-13-45H) = 0.60 g; $H_2$/CO = 2; $P$ = 3 MPa; $F$ = 30 mL $min^{-1}$; time on stream, 10 h.

$r$(CO) was caculated using the following equation:

$$r(\mathrm{CO}) = \frac{\mathrm{CO\ conv.\%} * F(\mathrm{CO}) * 60/22.4}{W(\mathrm{catalyst})}\ (\mathrm{mmol\ g^{-1}\ h^{-1}}).$$

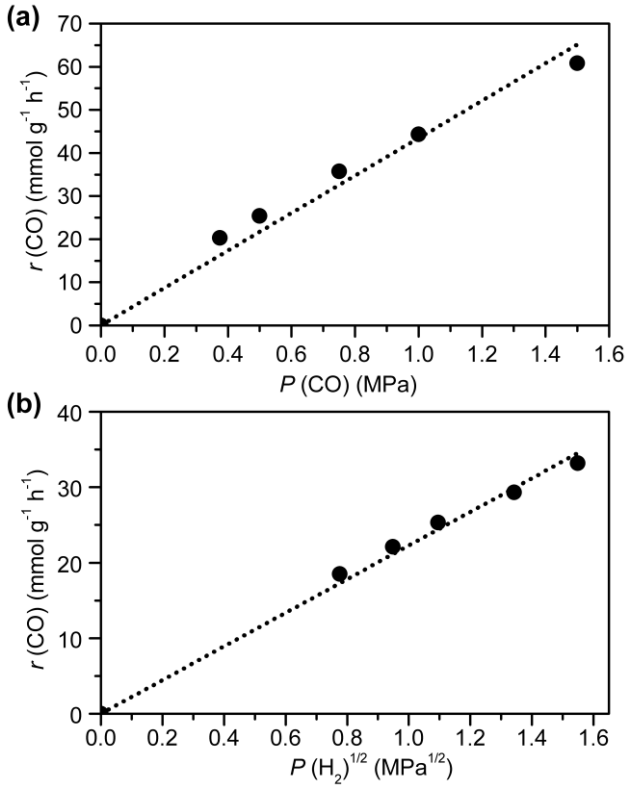


**Fig. S10** Rate of CO conversion versus CO and $H_2$ pressures. (a) $r$(CO) versus $P$(CO). (b) $r$(CO) versus $P(H_2)^{1/2}$.

The deviation from the linear relationship in each case indicates that the CO converion rate is less than first-order dependent on $P$(CO) (Fig. S10a) and slightly less than 0.5-order dependent on $P(H_2)$ (Fig. S10b).

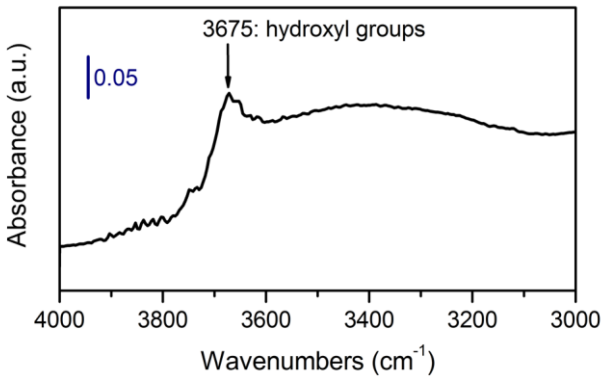


**Fig. S11** DRIFTS analysis of fresh Zn–$ZrO_2$ catalyst.

The Zn–$ZrO_2$ was pretreated in Ar flow at 673 K for 1 h, followed by cooling to 323 K under Ar. The spectrum was obtained by subtracting the background of KBr. The band at 3675 $cm^{-1}$ could be assigned to multi-coordinated hydroxyl groups.[7]

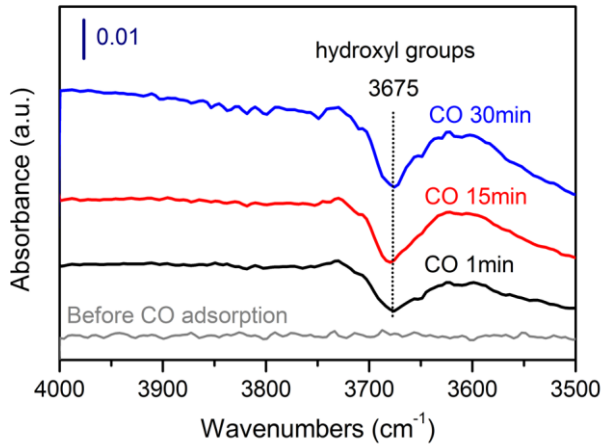


**Fig. S12** DRIFTS analysis of CO adsorption on Zn−$ZrO_2$ catalyst: evolution of surface hydroxyl groups after CO adsorption.

The Zn–$ZrO_2$ was pretreated in Ar flow at 673 K for 1 h, followed by cooling down to 553 K under Ar. The adsorption of CO was conducted at 553 K. The spectra were obtained by subtracting the background of Ar-pretreated Zn−$ZrO_2$ catalyst. The spectrum before CO adsorption was obtained by subtracting two backgrounds of Ar-pretreated catalyst. After the introduction of CO, a negative peak was observed. This indicates the consumption of multi-coordinated hydroxyl groups in the presence of CO.

**Table S3.** The WGS reaction under different $H_2O/CO$ ratios on $Zn-ZrO_2$ catalyst.[a]

| $H_2O/CO$[b] = *x* mL $min^{-1}$/ *y* mL $min^{-1}$ | $H_2O$ conversion (%) | CO conversion (%) |
|---|---|---|
| 10/10 | 50 | 50 |
| 5.0/10 | 79 | 39 |
| 2.5/10 | 91 | 18 |
| 1.2/10 | 94 | 11 |

[a] Reaction conditions: $W(Zn-ZrO_2)$ = 0.20 g, $T$ = 673 K, time on stream 10 h.

[b] Flow rates of $H_2O$ and CO.

**Table S4.** Estimated $CO_2$ selectivity by assuming thermodynamic equilibrium at different CO conversions.[a]

| Assumed CO conversion[b] (%) | $CO_2$ selectivity by thermodynamics (%)[c] |
|---|---|
| 10% | 45.9 |
| 20% | 45.5 |
| 30% | 45.1 |
| 40% | 44.6 |
| 60% | 42.9 |

[a] Assuming CO conversion follows a simplified $2H_2 + CO = H_2O + CH_2$ ($CH_2$ denotes olefins) and then a $H_2O + CO = CO_2 + H_2$ route. Reaction conditions used for simulation: $T$ = 673 K, $H_2/CO$ = 2:1 in the starting reactant. The calculation is based on HSC5 chemistry software.

[b] Assumed CO conversion integrates CO to olefins and the WGS reaction.

[c] The calculation of $CO_2$ selectivity is based on that the WGS reaction reaches equilibrium.

# 4. Reference


1. Z. Li, M. T. Navarro, J. Martinez-Triguero, J. Yu and A. Corma, *Catal. Sci. Technol.*, 2016, **6**, 5856-5863.
2. Y. Wang, A. P. Jia, M. F. Luo and J. Q. Lu, *Appl. Catal. B: Environ.*, 2015, **165**, 477-486.
3. D. A. Ward and E. I. Ko, *J. Catal.*, 1995, **157**, 321-333.
4. J. Datka, B. Gil and A. Kubacka, *Zeolites*, 1995, **15**, 501-506.
5. F. Yin, A. L. Blumenfeld, V. Gruver and J. J. Fripiat, *J. Phys. Chem. B*, 1997, **101**, 1824-1830.
6. G. V. A. Martins, G. Berlier, C. Bisio, S. Coluccia, H. O. Pastore and L. Marchese, *J. Phys. Chem. C*, 2008, **112**, 7193-7200.
7. M. Y. He and J. G. Ekerdt, *J. Catal.*, 1984, **87**, 381-388.